VISCOPLASTIC INSTABILITIES AND FAILURE OF DUCTILE MATERIALS

Alain Molinari, *Sébastien Mercier, Université de Lorraine, LEM3 (Laboratoire d'Etude des Microstructures et de Mécanique des Matériaux), UMR CNRS 7239, Ile du Saulcy, F-57045 Metz cedex 01, France. Téléphone : 03 87 31 53 60, Télécopie : 03 87 31 53 69, alain.molinari@univ-lorraine.fr, sebastien.mercier@univ-lorraine. Nicolas Jacques, ENSTA Bretagne, LBMS (Laboratoire Brestois de Mécanique et des Systèmes), EA 4325, 2 rue François Verny, F-29806 Brest cedex 9, France. nicolas.jacques@ensta-bretagne.fr.*

Mots clés : Ductile materials, viscoplastic flow instabilities, damage, dynamic failure, inertia.

1. INTRODUCTION

Dynamic failure of ductile materials is involved in a wide range of applications including the optimization of fast manufacturing processes and the security of structures exposed to impact, explosive loading or crash events. At high loading rates, tiny fluctuations in the plastic flow field induce important acceleration of material particles. Thus, significant inertia effects are taking place at the macroscopic level and sometimes also at the level of microscopic deformation mechanisms. Naturally, when subjected to dynamic loading the behavior of metallic materials is quite distinct from that observed under quasi-static conditions. The flow stress has higher rate dependence. The load bearing capacity is altered by thermal softening due to adiabatic heating resulting from plastic work. At last, inertia effects and material properties interact in a complex way that confers a dynamic signature to the patterning of plastic flow localization and to the process of internal damage.

Strain localization, which is often the precursor of failure of ductile materials, is the result of plastic flow instability, an outcome of geometrical or material softening. The patterning of strain localization is observed to be quite sensitive to the loading rate. A single neck is usually seen in a bar under quasi-static tensile loading while multiple necking is triggered at high stretching rates. Multiple necking is a true manifestation of inertia effects.

Fracture of ductile materials is often due to the nucleation, growth and coalescence of microscopic voids. Under dynamic loading conditions, these mechanisms can be substantially affected by inertia. The distinctive features of dynamic ductile damage are discussed in another presentation of this workshop (Jacques et al). A multiscale modelling of voided visco-plastic solids, incorporating micro-inertia effects, has been developped. The results suggest that considering microscale inertia is of primary importance in the modelling of spall fracture and dynamic ductile crack growth.

A comprehensive overview of the whole field of dynamic ductile failure is not attempted here. Selected topics of dynamic and quasistatic failure are presented here which comprise the analysis of: (i) dynamic necking and fragmentation, (ii) shear flow instabilities and adiabatic shear banding.

2. DYNAMIC NECKING

Experiments on metal rings and shells subject to intense stretching rates of the order of $10^4\ s^{-1}$ reveal that the fragmentation process of ductile materials is frequently initiated by multiple necking as illustrated in Fig.1, [1-5]. The following observations can be made:

- the number of necks and of fragments increases with the loading rate (Fig.1a)
- some necks are arrested before fracture (Fig.4b)
- the overall fracture strain is increasing with the loading rate (increased global ductility)

These features are intimately related to inertia effects.

2.1 Perturbation analysis

The early stages of multiple necking can be well captured by a linear stability approach. Perturbation methods were developed by Fressengeas and Molinari [6] and Mercier and Molinari [7-8] for the analysis of dynamic necking of viscoplastic materials. The quasistatic problem was examined by Hutchinson and Neale [9] and Hutchinson *et al* [10]. Dynamic necking of rate independent plastic materials was studied by Shenoy and Freund [11] and Guduru and Freund [12] by extending the quasistatic bifurcation analysis of Hill and Hutchinson [13]. Simplified one dimensional perturbation analyses with the Bridgman correction to account for multiaxial effects in necked regions have been also used, [14-17].

The effects of inertia are investigated here by following the development proposed by Mercier *et al* [2]. Results were obtained for a uniform plate subject to dynamic plane strain stretching and for incompressible visco-plastic materials obeying the J_2-flow theory and with flow stress of the form: $\sigma_Y = g(\varepsilon_e, \dot{\varepsilon}_e, T)$ with $\dot{\varepsilon}_e = \sqrt{(2/3) d_{ij} d_{ij}}$ and

$$\varepsilon_e(t) = \int_0^t \dot{\varepsilon}_e(\tau) d\tau \qquad (2.1)$$

$\dot{\varepsilon}_e$ is the effective plastic strain rate, d_{ij} is the plastic strain rate tensor, $\varepsilon_e(t)$ is the cumulated plastic strain at time t and T is the temperature. Strain hardening, strain rate hardening and thermal sensitivity are accounted for in the constitutive relation (2.1). Elastic deformations are neglected.

The plate occupies the domain defined by $-L_1 \le X_1 \le L_1$ and $-L_2 \le X_2 \le L_2$ in the initial reference configuration and is stretched in the direction X_1 with the constant velocity $\pm V$ applied at the extremities $X_1 = \pm L_1$, see Fig.2. We denote by l_1 the half current length, $\lambda = l_1 / L_1$ the longitudinal stretch.

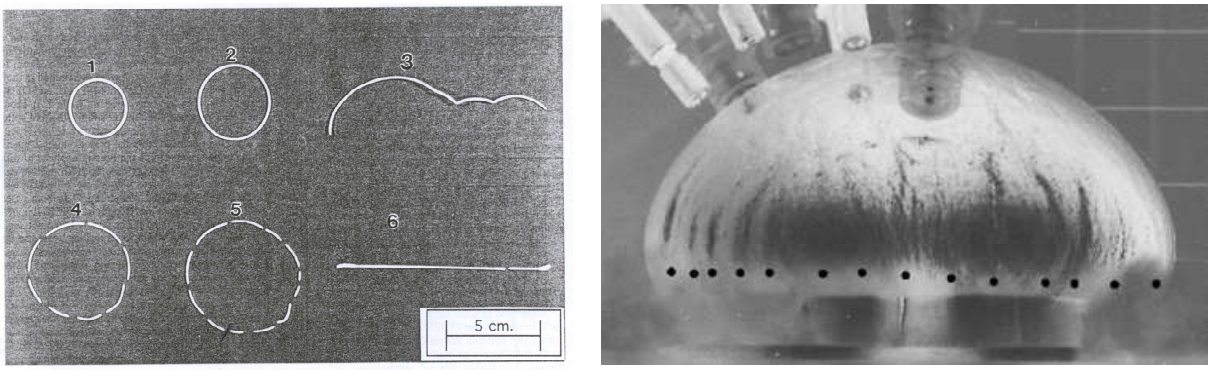

Fig. 1. (a) Necking and fragmentation of thin rings of solutionized 6061 Aluminum subject to rapid radial expansion by the effect of an intense magnetic field, Altynova et al [1]. The number of necks and the number of fragments increase with the energy input (i.e. with the stretching rate): 1) original, 2) 0.94 kJ, 3) 1.38 kJ, 4) 2.06 kJ, 5) 2.38 kJ, 6) quasistatic tensile test (single neck); (b) multiple necking of a tantalum hemisphere under rapid expansion (strain rates of the order of 10000 s^{-1}) by the effect of a shock loading generated by an explosive charge, Mercier et al [2].

The theoretical background solution that exists in absence of any flow instability can be calculated analytically [6] and involves lateral inertial effects. We denote by σ_e^0, ε_e^0, $\dot{\varepsilon}_e^0$ and T^0 respectively the flow stress ($\sigma_e = \sqrt{(3/2) s_{ij} s_{ij}}$ is the effective stress and s_{ij} the deviatoric stress), the cumulated plastic strain, the equivalent strain rate and the temperature of the background solution. These quantities are uniform. The evolution of T^0 results from adiabatic heating associated to plastic work.

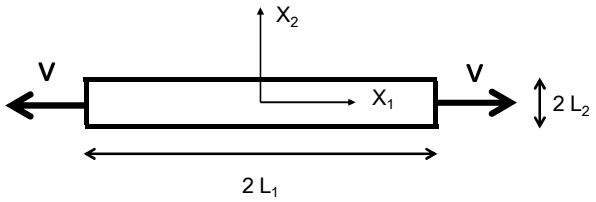

Fig. 2. Plate under plane strain deformation subject to the constant stretch-rate $\dot{\lambda} = V / L_1$

Plastic flow stability is analysed at any time t_* by perturbing the background solution with a small displacement field $\delta x_1(X_1, X_2, t)$, $\delta x_2(X_1, X_2, t)$ superimposed to the current position of material particles. (X_1, X_2) and (x_1, x_2) are respectively the Lagrangian and the Eulerian coordinates. The problem equations are linearized with respect to the corresponding disturbances of velocity, acceleration, strain-rates, cumulated plastic strain and stresses. To satisfy incompressibility of plastic flow a stream function, ϕ, is introduced such that $\delta x_1 = -\lambda \phi_{,2}$, $\delta x_2 = \lambda^{-1} \phi_{,1}$, where $(.)_{,i}$ is the partial derivative with respect to X_i.

The analysis investigates the exponential growth rate of modes of the form:

$$\phi(X_1, X_2, t) = A \exp(\eta(t - t_*)) \sin(kX_1) \exp(i\xi X_2) \qquad (2.2)$$

where η characterizes the time evolution, k and ξ are Lagrangian longitudinal and transversal wavenumbers. The boundary conditions at extremities are satisfied if $\sin(kX_1) = 0$ at $X_1 = \pm L_1$, i.e.:

$$kL_1 = j\pi \quad , \qquad (j \text{ positive integer}) \qquad (2.3)$$

The relationship between the growth rate η and the wave number k is obtained by using the lateral boundary conditions and can be written in terms of dimensionless parameters as:

$$\bar{\eta} = \bar{\eta}(\bar{p}_I / \bar{k}^2, \bar{k}, m, n / \varepsilon_e^0, q) \qquad (2.4)$$

with $$\bar{\eta} = \frac{\eta}{d_{11}} = \eta \frac{\lambda L_1}{V}, \qquad \bar{k} = kL_2 \lambda^{-2}, \qquad \bar{p}_I = \frac{\rho \dot{\lambda}^2}{\sigma_e^0} L_2^2 \lambda^{-4} \qquad (2.5)$$

m, n and q represent respectively strain rate sensitivity, strain hardening and thermal softening parameters. Inertia effects are embedded in the expression of the normalized inertial pressure $\bar{p}_I$.

This linearized perturbation approach was recently used to analyze multiple necking in the dynamic expansion experiments of hemispherical metallic shells, Fig.1b, Mercier *et al* [2].

2.2 Stabilizing effect of inertia.

Effects of inertia on the strain localization process can be illustrated by considering a rate dependent non-hardening material. The flow stress is taken as a power-law of the equivalent plastic strain rate:

$$\sigma_e = \sigma_R (\dot{\varepsilon}_e / \dot{\varepsilon}_R)^m \qquad (2.6)$$

The relationship (2.4) simplifies into $\bar{\eta} = \bar{\eta}(\bar{p}_I \bar{k}^{-2}, \bar{k}, m)$. Fig.3 shows results of the perturbation analysis for a plate of infinite length under plane strain stretching. The dependence of the normalized growth rate $\bar{\eta}$ is displayed in Fig.3a with respect to the normalized wave number $\bar{k}$ for $\lambda = 1$ (initial state) and the stretch-rate $\dot{\lambda} = 10^4 s^{-1}$. Material parameters are representative of copper and are reported in Table 1 together with loading conditions. A dominant instability mode is emerging with maximum growth rate $\bar{\eta}_{\max}$ and wave number $\bar{k}_{\max}$. The initial neck spacing is given by:

$$L_{neck} = 2\pi / k = 2\pi L_2 / \bar{k}_{\max} \qquad (2.7)$$

The quasistatic theory, obtained by setting $\bar{p}_I = 0$, indicates that $\bar{k}_{\max} = 0$, see Fig.3a, i.e. the neck spacing is infinite. For a plate of finite length, $\bar{k}_{\max}$ would correspond to the smallest value of the wave number compatible with the boundary conditions at $X_1 = \pm L_1$, i.e. j=1 in Eq.(2.3). Thus, in agreement with experimental results, a single neck is predicted by the quasistatic approach. Multiple

necking is clearly an outcome of inertia effects. The effect of the stretch-rate is illustrated in Fig.3b: $\bar{k}_{\max}$ increases with $\dot{\lambda}$. Consequently, the neck spacing decreases at higher stretch-rates according to Eq.(2.8) and the number of necks increases, as observed in Fig.1a.

Table 1. Material and loading parameters for the plate stretching problem

Material parameters		$\rho = 8900\ kg.m^{-3}$	$\sigma_R = 109\ MPa$
$\dot{\varepsilon}_R = 1\ s^{-1}$	$m = 0.05$		
Loading conditions	$\dot{\lambda} = 10^4 s^{-1}$	$L_2 = 0.3\ mm$	

Inertia stabilizes the strain localization process. By comparing the dynamic and quasistatic theories it is seen in Fig.3a that small wave-number modes (large wavelength) are slowed down by inertia. In addition, Fig.3b shows that the relative growth rate $\bar{\eta}_{\max}$ is a decreasing function of the stretch-rate. Therefore, necking is retarded by inertia at high loading rates.

The damping of short wave-length modes seen in Fig.3 is a consequence of stress multiaxiality as shown in [6-7] by comparing the complete 2-D theory to a simplified one dimensional dynamic approach developed by Fressengeas and Molinari [15]. Finally, the neck spacing appears to be (via the selection of a dominant instability mode) the outcome of the competition between material inertia that extinguishes long wavelength perturbations and stress multiaxiality effects that slow down short wavelength perturbations.

Recently, an extension of the classical linear stability analysis has been proposed by El Mai et al [45]. This approach allows for taking account of the contribution of all perturbation modes on the preliminary evolution of pre-necks. The distribution of pre-neck spacing could be characterized thus providing a deeper information as compared to the sole knowledge of the dominant neck spacing presented here.

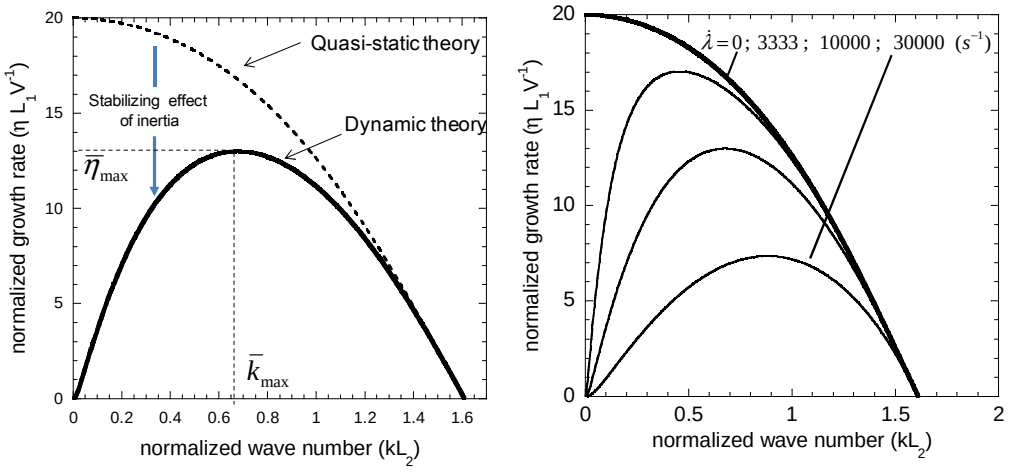

Fig. 3. (a) Normalized growth rate $\bar{\eta}$ in terms of the normalized wave number $\bar{k}$ =kL_2 in the initial state ($\lambda = 1$) for $\dot{\lambda} = 10^4 s^{-1}$. Material parameters are given in Table 1. The dominant mode is characterized by the wave number k_{max} and the normalized growth rate $\bar{\eta}_{max}$. With respect to the quasistatic theory, inertia slows down the long wavelength perturbations (small wave number) but has negligible effect on small wavelengths; (b) the number of necks is increases (larger $\bar{k}_{max}$) with the stretch-rate $\dot{\lambda}$ =V/L_1 as in Fig.1a, while the growth rate $\bar{\eta}_{max}$ decreases (neck retardation).

2.3 Neck retardation

It was qualitatively shown with the linearized perturbation analysis that, in addition to the usual retarding effects of strain hardening and strain rate hardening, strain localization could be strongly slowed down by inertia. This delay leads to the phenomenon of neck retardation which is considered as beneficial in terms of an overall increase of ductility. To quantify neck retardation one has to recourse to a fully non-linear analysis. Initial defects have an essential role in controlling the level of strain at which localized necking is triggered, [9]. Inertia effects and neck retardation due to inertia were explored by finite element simulations for bars under simple tension, [17-20], and for ring expansion tests, [21-23].

Xue *et al* [20] considered an infinite plate under plane strain constraint subject to the constant stretch-rate $\dot{\lambda}$. The flow stress is taken as rate-independent and given by the Hollomon law, $\sigma_e = \sigma_R \varepsilon_e^N$. They worked with periodic unit-cells to explore the effect of a geometrical defect (amplitude and wave-length), material parameters and inertia on strain localization and neck retardation. Finite element calculations were performed on unit-cells of the type shown in Fig.2, with $\dot{\lambda} = V / L_1$. The initial thickness of the plate, *h*, has a sinusoidal imperfection with initial wavelength, $L_w=2L_1$, and amplitude, η_0: $h=h^0(1-0.5\eta^0 \cos(2\pi X_1/L_w))$, with $h^0=2L_2$.

For several values of $\dot{\lambda}$, η^0 and L_w, Xue *et al* [20] calculated the overall strain at localized necking, $\bar{\varepsilon}_{Neck}$. They demonstrated the existence of a critical wavelength for which $\bar{\varepsilon}_{Neck}$ is minimized for given values of $\dot{\lambda}$ and η^0. This critical wavelength corroborates the emergence of a dominant instability mode suggested by the linearized stability analysis. The critical wavelength is a decreasing function of the applied stretch-rate, in qualitative agreement with the linearized stability analysis. Thus, the number of necks increases at high strain rates. The retarding effect of inertia on localized necking was also quantified by Xue et al [20], see Fig.4.

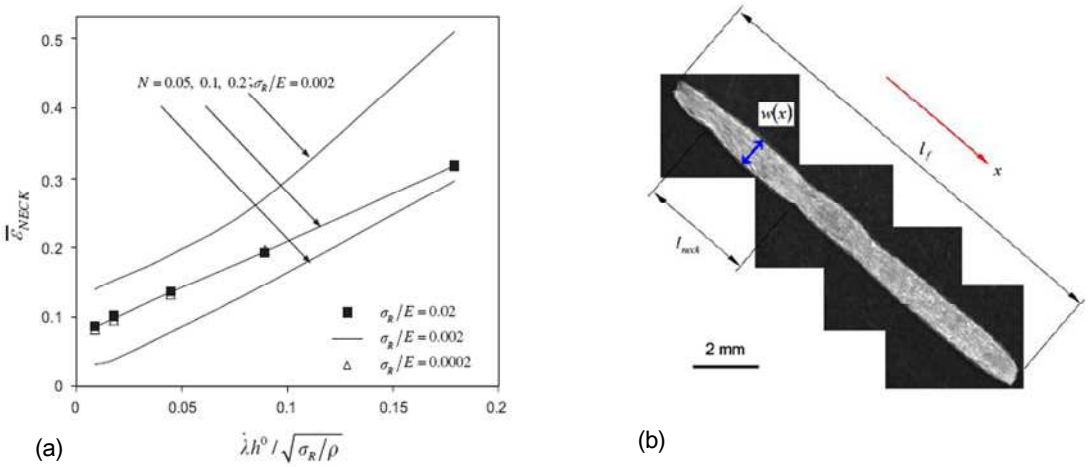

Fig. 4. (a) Results of the cell-model, Xue et al [20]. The necking strain $\bar{\varepsilon}_{Neck}$ increases with the normalized stretch-rate (neck retardation). The material response is rate-insensitive and described by the Hollomon law. Several hardening exponents, N, are considered. The amplitude of the geometrical defect is $\eta^0=0.04$. The effect of the Young modulus, E, appears to be negligible. (b) Arrested necks in a fragment of aluminum ring which was dynamically expanded, Zhang and Ravi-Chandar [5].

2.4 Fragmentation

The process of fragmentation of ductile rings subject to rapid expansion has been simulated with finite element calculations [24-26]. Zhou *et al* [16] have described the entire process of strain localization and fragmentation with a simplified one-dimensional framework using the Bridgman correction to account for stress multiaxiality within necked regions. The first stage is characterized by multiple necking with a characteristic neck pattern resulting from the selection of a dominant wavelength dictated by the interplay between inertia and material parameters. However, another

selection process is appearing later. When strain localization proceeds, it is observed that some necks are arrested while others are evolving to complete fracture. The phenomenon of neck arrest is clearly seen in the experiments of Zhang and Ravi-Chandar [5], Fig.4b, and in the numerical simulations of Zhou *et al* [16]. Slow necks are arrested by unloading Mott waves [27] emanating from fast growing necks.

The model of periodic unit-cells discussed in the previous section has a limitation since it assumes that the defects are periodically distributed along the sample (uniform wavelength and uniform imperfection amplitude). In this approach all necks develop equally and are equally spaced. If fracture is assumed to occur at the same failure strain, all necks would break simultaneously and none of them would be arrested. Thus, neck arrest is due to irregularities in the material properties and sample geometry. Consequently, statistical aspects are essential features of a fragmentation theory. Elegant and efficient theories of fragmentation based on statistical generation of fracture sites and occultation by unloading waves have been developed by Mott [27] and Grady [28]. However, in these approaches the material properties and defects are embedded in a "nucleation function" which governs the statistical generation of fracture sites. Actually, there is a need to link the fracture process to material and geometrical properties. The linearized stability analysis and the finite element simulations presented above are steps towards establishing this link, but further advances are still needed.

A simple heuristic view of the process of neck arrest can be attempted. For convenience, we assume that a constant overall strain rate $\dot{\varepsilon} = \dot{\lambda}/\lambda$ is applied instead of the constant stretch-rate $\dot{\lambda}$ as before. Consider two neighbour necks denoted as *Neck1* and *Neck2*. We neglect in a first step any interaction between necks and we denote by $\bar{\varepsilon}_{Fail}(1)$ (resp. $\bar{\varepsilon}_{Fail}(2)$) the value of the overall strain at which failure occurs within *Neck1* (resp. *Neck2*). Differences between $\bar{\varepsilon}_{Fail}(1)$ and $\bar{\varepsilon}_{Fail}(2)$ are due to fluctuations in material and geometrical defects. Failure strains can be calculated by using finite element computational cell-models accounting for the dynamic localization process and a failure criterion. Failure occurs within necks with a time delay δt_{Fail} which is roughly given by $\delta t_{Fail} = \delta\bar{\varepsilon}_{Fail}/\dot{\varepsilon}$, where $\delta\bar{\varepsilon}_{Fail} = \left|\bar{\varepsilon}_{Fail}(1) - \bar{\varepsilon}_{Fail}(2)\right|$. Denoting by L_{neck} the neck spacing, the time for the Mott unloading wave to travel with speed c_{Mott} from one neck to the next one is $\delta t_{Travel} = L_{neck}/c_{Mott}$. The slow neck is arrested if the unloading wave emanating from the fast neck arrives before completion of failure, i.e. if $\delta t_{Travel} < \delta t_{Fail}$. This analysis is certainly oversimplified, but it clearly indicates that the phenomenon of neck arrest is more likely to occur at low loading rates and for large fluctuations of the defect's amplitudes (leading to large $\delta\bar{\varepsilon}_{Fail}$), conditions under which large values of δt_{Fail} are expected. In the ideal case of a material and structure free of defects, we have $\delta\bar{\varepsilon}_{Fail} = 0$ and no neck is arrested.

When the loading rate $\dot{\varepsilon}$ is increased, $\delta t_{Fail} = \delta\bar{\varepsilon}_{Fail}/\dot{\varepsilon}$ is approaching zero, although $\delta\bar{\varepsilon}_{Fail}$ may be slightly growing with inertia effects. On the other hand it can be shown that L_{neck} is decreasing to a non-zero asymptotic limit at high strain rates, Rodriguez *et al* [29]. It follows that at high values of $\dot{\varepsilon}$ the characteristic unloading time $\delta t_{Travel} = L_{neck}/c_{Mott}$ tends to a non-zero limit, while δt_{Fail} is approaching zero. Therefore, the proportion of arrested necks is a decreasing function of $\dot{\varepsilon}$, as at high loading rates less time is left to the Mott unloading waves to communicate between necks. At very high strain rates, a situation is approached where all necks are fractured, and the fragment size is coming close to the neck spacing. Naturally the fragment size decreases with $\dot{\varepsilon}$ since the neck spacing and the number of arrested necks shrink with higher values of $\dot{\varepsilon}$.

To summarize, the fragmentation process is controlled by interplay between material properties, inertia and statistical defects. Inertia effects are more pronounced at higher strain rates (reduction of the neck spacing and fragment size, absence of communication between necks, increase of the overall ductility). Then, statistical defects are getting less important and the problem turns out to be more deterministic.

It is worth mentioning that similar conclusions are reached when dealing with multidimensional dynamic fracture of ductile materials (Grady [28]) or when considering brittle materials (Denouald

and Hild [30], Forquin and Hild [31]) although the failure mechanics are quite different (necking versus micro-cracking).

3. ADIABATIC SHEAR BANDING

Ductile failure by adiabatic shear banding is frequently observed in metals subject to high loading rates especially when compressive and shearing modes are involved. Adiabatic shear bands (ASB) are seen in impact and penetration problems. They are also involved in fast forming processes such as forging and high speed machining. ASB are narrow zones with thickness of the order of few micro-meters where shear deformation is highly localized. Here again, the process of strain localization is a consequence of plastic flow instability, generally attributed to thermal softening due to heating by plastic work and quasi-adiabatic conditions. However, for some materials, other softening mechanisms such as dynamic recrystallization or phase transformation may be involved, see for instance Rittel *et al* [32]. Reviews on ASB can be found in Bai and Dodd [33] and Wright [34].

The spontaneous occurrence of a family of ASB and their collective behavior can be experimentally captured by considering the radial collapse of cylinders driven by explosive loading, Nesterenko *et al* [35] or electromagnetic pulses, Lovinger *et al* [36]. It is of interest to note that families of ASB with regular spacing are also observed in high speed machining of metals (chip segmentation) where shearing is the main deformation mode, Komanduri and Von Turkovich [37], Molinari et al [38], Miguelez et al [39], Molinari et al [40].

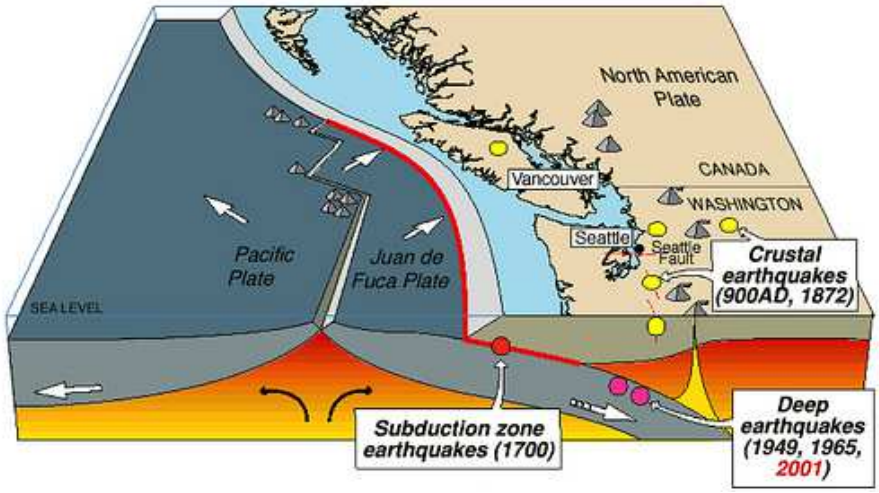

Fig.5: Earthquakes at the interface of the Juan de Fuca and North American plates (www.pnsn.org/outreach/earthquakesources).

There is a strong similarity between the analysis of dynamic necking in expanding rings and shells and adiabatic shear banding in collapsing cylinders, with however some important differences. Geometrical softening is not playing any role in the case of ASB. Instead, shear localization is driven by thermal softening and short wavelength perturbations are damped by heat diffusion. Similarly to the problem of multiple necking, higher strain rates promote inertia effects that are conducive to multiple shear banding and to a decreasing of the shear band spacing and fragment size. The shear band spacing was characterized by using perturbation approaches by Wright and Ockendon [41] for viscoplastic response with no-strain hardening and by Molinari [42] for strain-hardening materials. Recently, the fragmentation process associated to adiabatic shearing was addressed by Zhou *et al* [43] with the type of approach developed by Zhou *et al* [16] to investigate fragmentation by multiple necking. It was shown that the early stage of the localization process is well described with the linear stability analysis. The entire process of fragmentation, including shear band generation and growth as well as shear band arrest by unloading waves was described with non-linear calculations. The

spacing between mature (non arrested) shear bands was found to be closer to that predicted by the momentum diffusion theory of Grady and Kipp [44] than by the linearized stability approach.

Finally we will investigate the occurrence of shear flow instabilities in geophysical sciences. We will consider subduction zones that could be at the site of either deep earthquakes, [46], or slow slip events, see Fig.5. Recent results obtained by Mercier, Molinari and Avouac [47] will be discussed.

4 CONCLUSION

We have seen that inertia can deeply act upon the mechanisms of dynamic ductile failure of metallic materials. The mark of inertia was recognized at the macro-scale and micro-scale levels and can bear different aspects:

- Long wavelength perturbations and large scale defects are damped by inertia. Thus, the characteristic spacing between localization, fracture and damage sites is reduced at higher loading rates.
- The growth rate of perturbations and imperfections is slowed down by inertia. Therefore, strain localization is retarded at high strain rates. This results in an increase of the apparent overall ductility.
- Wave propagation phenomena are important aspects of dynamic failure. Dynamic failure can be triggered by wave interaction (spalling) or inhibited by unloading waves during fragmentation processes.

In addition, we have discussed how thermal effects can substantially affect shear flow localization in metallic materials subjected to high strain rates (impact and high speed forming processes) and in geophysical sciences (deep earthquakes and slow slip events in subduction zones).

References

[1] Altynova M, Hu X, Daehn GS. Increased ductility in high velocity electromagnetic ring expansion. *Metall Trans A* 1996;**27**:1837–44.

[2] Mercier S, Granier N, Molinari A, Llorca F, Buy F. Multiple necking during the dynamic expansion of hemispherical metallic shells, from experiments to modeling. *J Mech Phys Solids* 2010;**58**:955–982.

[3] Niordson FL. A unit for testing materials at high strain rates. *Exp Mech* 1965;**5**:29–32.

[4] Grady DE, Benson DA. Fragmentation of metal rings by electromagnetic loading. *Exp Mech* 1983;**12**:393–400.

[5] Zhang H, Ravi-Chandar K, On the dynamics of necking and fragmentation: I. Real-time and post-mortem observations in Al6061-O. *Int J Fract* 2006;**142**:183–217.

[6] Fressengeas C, Molinari A. Fragmentation of rapidly stretching sheets. *Eur J Mech A/Solids* 1994;**13**:251–68.

[7] Mercier S, Molinari A. Predictions of bifurcation and instabilities during dynamic extension. *Int J Solids Struct* 2003;**40**:1995–2016.

[8] Mercier S, Molinari A. Analysis of multiple necking in rings under rapid radial expansion. *Int J Impact Eng* 2004;**30**:403–419.

[9] Hutchinson JW, Neale KW. Influence of strain-rate sensitivity on necking under uniaxial tension. *Acta Metall* 1977;**25**:839–846.

[10] Hutchinson JW, Neale KW, Needleman A. Sheet necking—I. Validity of plane stress assumptions of the long wavelength approximation. In: Koistinen, D.P., Wang, N.-W. (Eds.), *Mechanics of Sheet Metal Forming*, New York: Plenum Publishing Corp; 1978, p.111–126.

[11] Shenoy VB, Freund LB. Necking bifurcations during high strain rate extension. *J Mech Phys Solids* 1999;**47**:2209–33.

[12] Guduru PR, Freund LB. The dynamics of multiple neck formation and fragmentation in high rate extension of ductile materials. *Int J Solids Struct* 2002;**39**:5615–32.

[13] Hill R., Hutchinson JW. Bifurcation phenomena in the plane tension test. *J Mech Phys Solids* 1975;**23**:239–264.

[14] Walsh JM. Plastic instability and particulation in stretching metals jets. *J Appl Physics* 1984;**56**:1997–2006.

[15] Fressengeas C, Molinari A. Inertia and thermal effects on the localization of plastic flow. *Acta Metall* 1985;**33**:387–396.

[16] Zhou F, Molinari JF, Ramesh K. An elastic-visco-plastic analysis of ductile expanding ring. *Int J Impact Eng* 2006;**33**:880–891.

[17] Vadillo G, Rodriguez-Martinez JA, Fernandez-Saez J. On the interplay between strain rate and strain rate sensitivity on flow localization in the dynamic expansion of ductile rings. *Int J Solids Struct* 2012;**49**:481–491.

[18] Needleman A. The effect of material inertia on neck development. In: Yang WH, editors. *Topics in Plasticity*, Ann Arbor MI: AM Press; 1991, p.151–160.

[19] Knoche P, Needleman A. The effect of size on the ductility of dynamically loaded tensile bars. *Eur J Mech* 1993;**12**:585-601.

[20] Xue Z, Vaziri A, Hutchinson J, Material aspects of dynamic neck retardation. *J Mech Phys Solids* 2008;**56**:93–113.

[21] Tugcu P, Neale KW, Lahoud AE. Inertial effects on necking in tension. *Int J Solids Struct* 1990;**26**:1275–1285.

[22] Han JB, Tvergaard V. Effect of inertia on the necking behaviour of ring specimens under rapid expansion. *Eur J Mech A/Solids* 1995;**14**:287–307.

[23] Sorensen NJ, Freund LB. Unstable neck formation in a ductile ring subjected to impulsive radial loading. *Int J Solids Struct* 2000;**37**:2265–83.

[24] Becker R. Ring fragmentation predictions using the Gurson model with material stability conditions as failure criterion. *Int J Solids Struct* 2002;**39**:3555–3580.

[25] Rusinek A, Zaera R. Finite element simulation of steel ring fragmentation under radial expansion. *Int J Impact Eng* 2007;**34**:799–822.

[26] Pandolfi A, Krysl P, Ortiz M. Finite element simulation of ring expansion and fragmentation: the capturing of length and time scales through cohesive models of fracture. *Int J Fract* 1999;**95**:279–297.

[27] Mott N. Fragmentation of shell cases. *Proc Royal Soc Series A* 1947;**189**:300–308.

[28] Grady D. *Fragmentation of Rings and Shells*. Berlin Heidelberg: Springer; 2006.

[29] Rodriguez-Martinez JA, Vadillo G, Fernandez-Saez J, Molinari A. Identification of the critical wavelength responsible for the fragmentation of ductile rings expanding at very high strain rates (submitted).

[30] Denouald C, Hild F. Dynamic fragmentation of brittle solids: a multi-scale model. *Eur J Mech A/Solids* 2002;**21**:105-120.

[31] Forquin P, Hild F. A probabilistic damage model of the dynamic fragmentation process in brittle materials. *Adv Appl Mech* 2010;**44**:1-71.

[32] Rittel D, Landau P, Venkert A. Dynamic recrystallization as a potential cause of adiabatic shear failure. *Phys Rev Letters* 2008; article number 165501.

[33] Bai Y, Dodd B. *Adiabatic shear localization*. Oxford: Pergamon; 1992.

[34] Wright TW. *The physics and mathematics of adiabatic shear bands*. Cambridge: Cambridge Univ Press; 2002.

[35] Nesterenko VF, Meyers MA, Chen HC, LaSavia JC. Controlled high-rate localized shear in porous reactive media. *Appl Phys Lett* 1994;**65**:3069-3071.

[36] Lovinger Z, Rikanati A, Rosenberg Z, Rittel D. Electro-magnetic collapse of thick-walled cylinders to investigate spontaneous shear localization. *Int J Impact Eng* 2011;**38**:918-929.

[37] Komanduri R, Von Turkovich BF. New observations on the mechanism of chip formation when machining titanium alloys. *Wear* 1981;**69**:179-88.

[38] Molinari A, Musquar C, Sutter G. Adiabatic shear banding in high speed machining of Ti-6Al-4V : experiments and modelling. *Int. J. of Plasticity* 2002;**18**, 443-459.

[39] Miguelez MH, Soldani X, Molinari A. Analysis of adiabatic shear banding in orthogonal cutting of Ti alloy *Int J. Mech Sciences* 2013; **75**, 212-222.

[40] Molinari A, Soldani X, Miguelez MH. Adiabatic shear bandingand scaling laws in chip formation with application to cutting of Ti-6Al-4V *J. Mech Phys Solids* 2013;**61**, 2331-2359.

[41] Wright TW, Ockendon H. A scaling law for the effect of inertia on the formation of adiabatic shear bands. *Int J Plasticity* 1996;**12**:927-934.

[42] Molinari A. Collective behavior and spacing of adiabatic shear bands. *J Mech Phys Solids* 1997;**45**:1551-75.

[43] Zhou F, Wright TW, Ramesh KT. The formation of multiple adiabatic shear bands. *J Mech Phys Solids* 2006;**54**:1376-1400.

[44] Grady DE, Kipp ME. The growth of unstable thermoplastic shear with application to steady-wave shock compression in solids. *J Mech Phys Solids* 1987;**35**:95-119.

[45] El Maï S., Mercier S., Petit J., Molinari A. An extension of the linear stability analysis for the prediction of multiple necking during dynamic extension of round bar. *Int. J. of Solids and Structures* 2014; **51**:3491-3507.

[46] Kameyama M. Comparison between thermal-viscous coupling and frictional sliding. *Techtonophysics 2003;* **376**, 185-197.

[47] Mercier S, Molinari A, Avouac JP. Ductile shear instabilities due to thermo-mechanical coupling, a possible cause for periodic slow slip events, submitted.